
Production Systems and Information Engineering
Volume 13 (1), pp. 41–52.
https://doi.org/10.32968/psaie.2025.1.4

SEARCH ALGORITHM FOR DETERMINING THE ILLUMINATION FREQUENCY IN A LINE SCAN CAMERA-BASED MEASUREMENT SYSTEM

ZSÓFIA FORGÁCS
University of Miskolc
Hungary Institute of Automation and Infocommunication
zsofia.forgacs@uni-miskolc.hu

Abstract: At the University of Miskolc, a machine vision-based measurement system was developed utilizing a line scan camera to capture images line by line as the object moves. A critical challenge in such systems is synchronizing the camera's exposure frequency with the lighting control pulse train. Discrepancies between these two frequencies could lead to periodic intensity variations in the image. To address this issue, a frequency search algorithm was developed. This algorithm compensates for differences between the camera's exposure signal and the lighting control signal, preventing resonance and intensity fluctuations. The paper details the algorithm's operation and related preliminary investigations.

Keywords: *line scan camera, exposure, illumination control, signal processing*

1. Introduction

At the University of Miskolc, a machine vision-based measurement system was previously developed, utilizing a line scan camera for image capture [1]. Line scan cameras operate by recording one line of an image at a time, and as the object moves or rotates, the camera builds up a complete image by sequentially recording these lines. A key parameter of these cameras is the line rate, which determines the number of lines that can be captured per second. This is crucial for ensuring that the camera can keep up with the speed of the moving object [2, 3, 4]. Additionally, the illumination frequency must be set appropriately to avoid image artifacts such as flickering or inconsistent lighting, which could distort the accuracy of the measurement. Proper synchronization between the camera's line rate and the light source is essential for capturing high-quality, distortion-free images.

The performance of measurement systems relying on machine vision is significantly affected by the lighting approach employed [5, 6]. Line-scan cameras sensor area is considerably smaller compared to conventional area-scan cameras.

Consequently, when designing the illumination, the geometry of the lighting unit is not the primary consideration, rather, a simple line-lighting arrangement is suitable. A more crucial factor is that due to the brief exposure times, the camera requires a higher light intensity to acquire sufficient illumination for image formation.

Many industrial cameras can provide the active exposure duration during image acquisition [7], enabling the synchronization of lighting with the exposure. This allows, for instance, the implementation of pulse-controlled LED illumination. The advantage of pulse control mode is the extended lifetime of the LED, as it is powered for a shorter duration per unit of time, resulting in reduced heat generation. Since traditional lighting control using the camera output signal does not provide feedback on the recorded and processed image data, an alternative lighting method was developed. An independent lighting control unit offers the capability to feed back the image data, thereby regulating the control signal of the LED light sources.

The camera exposure signal and the LED pulse train originate from distinct sources, resulting in uncertainty regarding their synchronization. If the exposure signal and the lighting control signal share the same frequency, their complete overlap can be guaranteed by adjusting the phase shift of the latter. Nevertheless, in practical applications, the sampling frequency of the camera and the frequency of the signal provided by the lighting controller may diverge, potentially leading to resonance and fluctuations in the recorded image intensities.

To comprehend this phenomenon and develop a frequency difference compensation algorithm, a procedure was established. This procedure enables the estimation of the intensity arising from the overlap of the signal curves for each pixel row based on the two signals. Using this simulation, a method was devised to compensate for the frequency difference.

The previously developed simulation algorithm was utilized to conduct measurements aimed at determining the accuracy of the frequency difference between the camera exposure and the lighting control signal. Analysis of the obtained measurement results revealed the necessity to develop a frequency search algorithm. This paper outlines the operation of the algorithm and the associated examinations.

2. Examination of the Determinability of the Frequency Difference

The lighting frequency can be regulated based on the periodic intensity changes observed in the recording, provided that the frequency difference can be characterized. The investigation began with an examination of the transition length in the intensity curve. Specifically, the study investigated how the transition length, denoted as Δx, varies in relation to the line rate and the discrepancy between the set and actual frequencies, as detailed in the following data.

- Line rate [Hz]: $\mathrm{X} = \{f_i \mid 1000 + f_i \cdot 500, where\ i = 0, 1, 2, \dots, 97\}$

- Frequency difference [Hz]: $\mathrm{Y} = \left\{ \begin{matrix} \Delta f_j \mid \Delta f_j = j - 500, \\ where\ j = 0, 1, 2, \ldots, 1000 \end{matrix} \right\}$
- Transition length [px]: $\mathrm{Z} = \{\Delta x_{ij}\}$

The value of Δx was determined with Equation 1.

$$\Delta x = \delta \cdot \left(max\_index_O - (|R| - index_{R'})\right) + (1 - \delta) \cdot \left(min\_index_O - (|R| - index_{R'})\right), \quad (1)$$

$where$

$$\delta = \begin{cases} 0, if\ max\_index_O \leq min\_index_O\ (descending) \\ 1, if\ max\_index_O > min\_index_O\ (rising) \end{cases},$$

$$min\_index_O = \min(j \mid 0 \leq j < H \wedge O[j] = \min(O)),$$

$$max\_index_O = \min(j \mid 0 \leq j < H \wedge O[j] = \max(O)),$$

$$|R| = \delta \cdot (max\_index_O + 1) + (1 - \delta) \cdot (min\_index_O + 1),$$

$$index_{R'} = \min(i \mid R'[i] = \delta \cdot \min(R') + (1 - \delta) \cdot \max(R')),$$

$$R = \{O[j] \mid 0 \leq j \leq \delta \cdot max\_index_O + (1 - \delta) \cdot min\_index_O\},$$

$$R'[i] = \{R[\delta \cdot max\_index_O + (1 - \delta) \cdot min\_index_O - i] \mid i \in \{0, 1, \ldots, |R| - 1\}\}.$$

The length of the transition as a function of the frequency difference can be seen in Figure 1 on an $H = 1024$ pixel high image.

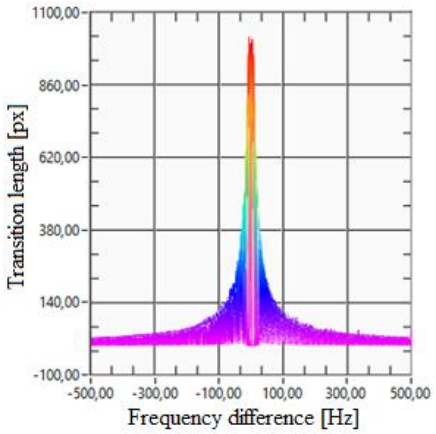

Figure 1. The length of the transition based on the frequency difference

The Lorentz function, frequently used to model resonance phenomena [8], can accurately capture the amplitude peaks and resonance width. The function's shape, determined by the transition length Δx, frequency difference Δf, line rate f_s, and damping factor γ, can be represented by Equation 2 on an image with a height of H pixels.

$$\Delta x = \left(\frac{H-1}{\pi}\right) \cdot \frac{|\Delta f|}{\sqrt{\Delta f^2 + \left(\frac{\gamma(f_s)}{2}\right)^2}} \tag{1}$$

The absolute difference in frequency values was determined to be:

$$|\Delta f| = \sqrt{\frac{-\Delta x^2 \cdot \left(\frac{\gamma(f_s)}{2}\right)^2}{\Delta x^2 - \left(\frac{H-1}{\pi}\right)^2}} \tag{2}$$

By incorporating the correction factor $\gamma(f_s)$, we account for the effect that variations in the line rate have on the simulation results. A potential approximation of this relationship can be described using parameters γ_0, k, and m, which can be determined based on the simulation data:

$$\gamma(f_s) = \gamma_0 + k \cdot {f_s}^m \tag{3}$$

During the search for the optimal approximation, the algorithm produced an average error exceeding 10% upon evaluation. The approximation technique can be improved by employing $\gamma(f_s)$ as a complex function and incorporating additional terms $k \cdot {f_s}^m$ as specified in Equation 5.

$$\gamma(f_s) = \gamma_0 + k_1 \cdot {f_s}^{m_1} + k_2 \cdot {f_s}^{m_2} + \cdots + k_n \cdot {f_s}^{m_n} \tag{4}$$

Further research was conducted on other characteristics of the intensity curve, such as the slope of the rise and fall. However, it was concluded that the computational requirements for determining the frequency difference were prohibitively expensive compared to the achievable accuracy. Consequently, the goal was to implement a control method based on a more easily implementable and cost-effective search algorithm.

3. Development of the Frequency Search Algorithm

The proposed frequency search algorithm aims to determine the frequency f_g of the lighting control signal, at which the average of the recorded intensity values is closest to the value of I_{max}, the maximum intensity. Here, the mean of the vector 0 is 1 and the variance value is 0. Variance, a measure of the dispersion or variability of a variable within a data matrix, indicates the degree to which the values deviate from the mean. The column with the largest variance is considered the most variable. Variance (σ^2) can be expressed using Equation 6, where N is the sample number, X_i is the current value, and μ is the average of the sample.

$$\sigma^2 = \frac{1}{N}\sum (X_i - \mu)^2 \tag{5}$$

The algorithm iterates through a specified frequency range, adjusting the lighting control signal in discrete step intervals. Throughout this process, it continuously computes the mean and variance of the vector O, which contains the overlap ratios. At each frequency within the defined range, the algorithm performs multiple tests to gather more accurate data.

The search algorithm is triggered when the mean of the O vector exceeds a given threshold, $K_\mu < \overline{O}$, while the variance remains below another threshold, $K_{\sigma^2} > \sigma^2(O)$. Once these conditions are met, the algorithm systematically increases the frequency of the lighting control signal according to Equations 7 and analyzes the resulting data.

$$
\begin{aligned}
n_f[i+1] &= \begin{cases} 0, if\ n_f[i]+1 \geq N_f \cdot N_r \\ n_f[i]+1, otherwise \end{cases} \\
n_r[j+1] &= \begin{cases} 0, if\ n_r[j]+1 \geq N_r \\ n_r[j]+1, otherwise \end{cases} \\
f_g[k+1] &= \begin{cases} f_g[0], if\ n_f[i]+1 \geq N_f \cdot N_r \\ f_g[k], if\ n_r[j]+1 \geq N_r \\ f_g[0] - \dfrac{N_r \cdot \Delta f_g}{2} + \Delta f_g \cdot \left\lfloor \dfrac{n_f[i]+1}{N_r} \right\rfloor, otherwise \end{cases} \\
\mu[k+1] &= \overline{O} \\
\sigma^2[k+1] &= \sigma^2(O)
\end{aligned}
\tag{6}
$$

where

n_f: number of measurement cycles at the given frequency,
N_f: maximum number of different frequencies,
n_r: the number of repetitions within the given frequency,

N_r: the maximum number of repetitions within the given frequency,
Δf_g: frequency step,
μ: vector of mean values $\overline{O}$[j],
σ^2: the vector of variance values σ^2(O[j]).

Figure 2 shows the result of a run with the set parameters $N_f = 100$, $N_r = 5$, $\Delta f_g = 1\,Hz$ and $f_g[0] = 9992\,Hz$, while the line rate f_s to be searched for is 10 kHz.

If the condition $n_r[k] + 1 \geq N_r$ is met, the algorithm assesses the data of the vectors μ and σ^2. Examination of the frequencies reveals the formation of a broad peak on the curve of the average values, suggesting the presence of values close to the sought frequency of 10 kHz. The aim is to identify the center of this peak, as this point represents the highest average intensity values and the minimum of the variance values.

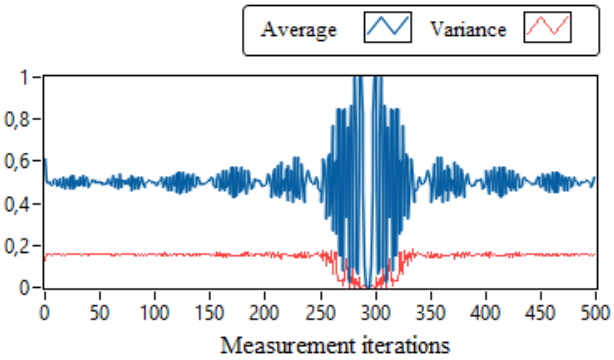

Figure 2. *Result of the frequency search algorithm*

To analyze the curve depicting the average values, the amplitude values of the curve $A(\mu_k) = [A(\mu_1), A(\mu_2), \dots, A(\mu_m)]$ were calculated using the following relation:

$$A(\mu_k) = \begin{cases} \mu_k, if\ \mu_k \geq \dfrac{\max(\mu) + \min(\mu)}{2} \\ \max(\mu) + \min(\mu) - \mu_k, if\ \mu_k < \dfrac{\max(\mu) + \min(\mu)}{2} \end{cases} \tag{7}$$

In order to smooth the amplitude curve, its values were averaged and added to the vector $B = [B_1, B_2, \dots, B_{m-n+1}]$ according to Equation 9.

$$B_k = \frac{1}{n} \cdot \sum_{i=k-n+1}^{k} A(\mu_i), if\ k \geq n \tag{8}$$

The graphical representation of the values associated with vectors A and B, as produced through this method, is illustrated in Figure 3.

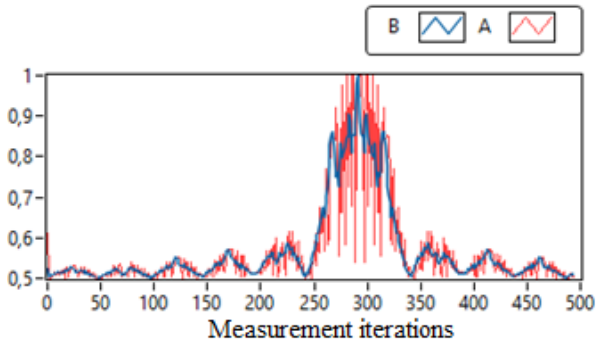

Figure 3. *Amplitude and average of the mean value curve*

The developed algorithm identifies the center point c of the curve peak by searching for the iterations with the smallest and largest index where the B vector values exceed a specified threshold. The algorithm then calculates the arithmetic mean of these two index values to determine the center point. Similarly, the threshold used to locate the peak is established by computing the arithmetic mean of the largest and smallest average values, as described in Equation 10.

$$c_0 = \frac{i_{min} + i_{max}}{2}, \text{where:}$$
$$i_{min} = \min\left\{i \mid B_i > \frac{\max(\mu_B) + \min(\mu_B)}{2}\right\} \quad (9)$$
$$i_{max} = \max\left\{i \mid B_i > \frac{\max(\mu_B) + \min(\mu_B)}{2}\right\}$$

When the target frequency is identified during the first or final iterations, the examined waveform lacks a complete peak, as demonstrated by the data series depicted in Figure 4, with parameter settings of $N_f = 50$, $N_r = 5$, $\Delta f_g = 1\ Hz$, and $f_g[0] = 10024\ Hz$, and a line update frequency of 20 kHz.

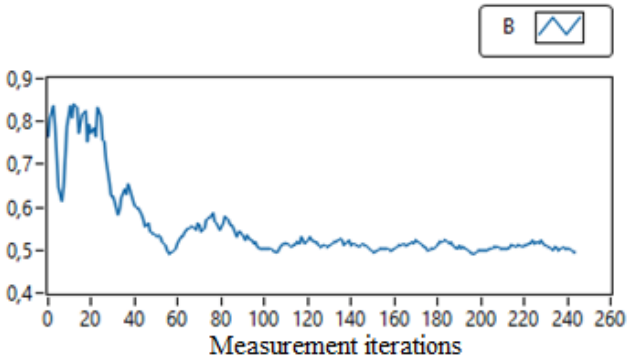

Figure 4. *Average values when the target frequency is found in the outer iterations*

In this case, a new search can be run with modified input parameters of the search algorithm. Figure 5 shows an example of this by increasing the number of measurement iterations to $N_f = 100$.

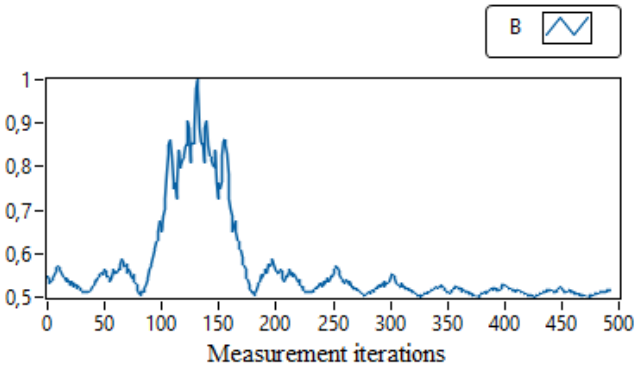

Figure 5. *Average values with increased number of iterations*

The selection result of point c_0 can be refined by examining the variance values in the neighborhood of the point, in the range $[i_{min}, i_{max}]$. This check is performed if the variance for the average value selected on curve B is greater than 0, because then a change in intensity can be assumed in the recording. During the test, the measurement iteration indices where the variance is minimal can be determined with Equation 11, and then the point c closest to c_0 is selected from among them.

$$i_{min\_var} = \{j \mid i_{min} \le j \le i_{max}, \sigma^2(j) = \min(\sigma^2(i))\}$$
$$c = \begin{cases} c_0, if\ \sigma^2(c_0) = 0 \\ i \mid i \in i_{min\_var}, |i - c_0| = \min(|j - c_0| \mid j \in i_{min\_var}), otherwise \end{cases} \quad (10)$$

4. Results

The frequency search algorithm was tested using the previously developed simulation algorithm. The evaluation of the tests utilized the relative error of the specified frequency reference signal compared to the line rate. The input parameters and results of different test runs are summarized below.

Case 1: $N_f = 50$, $N_r = 5$, $\Delta f_g = 1$ Hz, $f_s = \mathrm{i} \cdot 10$ kHz and $\Delta f = \mathrm{j} \cdot 1$ Hz, where $i \in \{1, 2, 3, 4, 5\}$ and $j \in \{1, 2, \ldots, 10\}$. The performance of the system was examined under 5 different line rates ranging from 10 kHz to 50 kHz, and 10 different frequency differences from 1 Hz to 10 Hz, with a step size of 1 Hz. This resulted in a total of $5 \cdot 50 = 250$ measurements performed in each ij cycle iteration. The relative error of the calculated frequency setpoint is depicted in Figure 6.

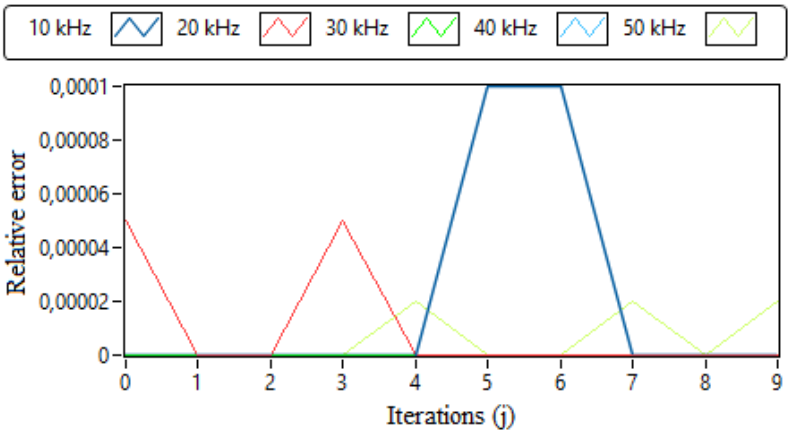

Figure 6. *The first test results of the search algorithm*

Table 1 details the run results.

Table 1

Relative error values [%] in the 1st test cycle

Δf: \ f_s:	**10 kHz**	**20 kHz**	**30 kHz**	**40 kHz**	**50 kHz**
1	0	0.005	0	0	0
2	0	0	0	0	0
3	0	0	0	0	0
4	0	0.005	0	0	0
5	0	0	0	0	0.002
6	0.01	0	0	0	0
7	0.01	0	0	0	0
8	0	0	0	0	0.002
9	0	0	0	0	0
10	0	0	0	0	0.002

At lower line rates, enhancing the number of repetitions (N_r) per frequency can improve the accuracy of the measurements. Consequently, for the subsequent experiment, the test parameters were adjusted accordingly.

Case 2: $N_f = 50$, $N_r = 10$, $\Delta f_g = 1$ Hz, $f_s = \mathrm{i} \cdot 10$ kHz és $\Delta f = \mathrm{j} \cdot 1$ Hz, ahol $i \in \{1, 2, 3, 4, 5\}$ és $j \in \{1, 2, \ldots, 10\}$. Five distinct line update frequencies ranging from 10 to 50 kHz, and ten frequency differences from 1 to 10 Hz in 1 Hz

increments, were investigated during the testing process. A total of 500 measurements were performed in an iterative ij cycle. The outcomes of the second test cycles are presented in Figure 7 and Table 2.

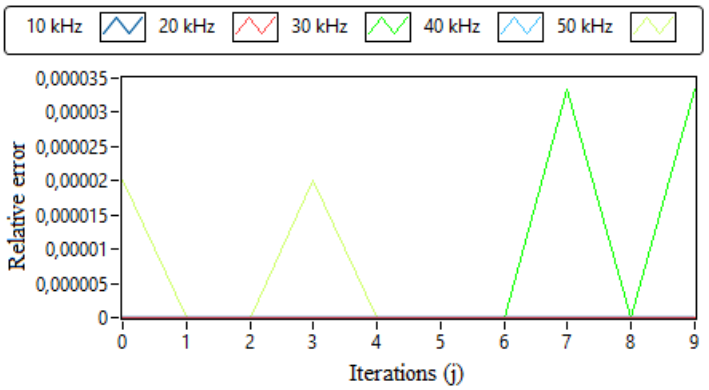

Figure 7. *The second test results of the search algorithm*

Table 2

Relative error values [%] in the 2nd test cycle

Δf: \ f_s:	**10 kHz**	**20 kHz**	**30 kHz**	**40 kHz**	**50 kHz**
1	0	0	0	0	0.002
2	0	0	0	0	0
3	0	0	0	0	0
4	0	0	0	0	0.002
5	0	0	0	0	0
6	0	0	0	0	0
7	0	0	0	0	0
8	0	0	0.0033	0	0
9	0	0	0	0	0
10	0	0	0.0033	0	0

Case 3: $N_f = 100$, $N_r = 10$, $\Delta f_g = 1$ Hz, $f_s = \mathrm{i} \cdot 10$ kHz és $\Delta f = \mathrm{j} \cdot 1$ Hz, ahol $i \in \{1, 2, 3, 4, 5\}$ és $j \in \{1, 2, \dots, 10\}$. The testing process involved examining five distinct line update frequencies ranging from 10 to 50 kHz, and ten frequency differences from 1 to 10 Hz in 0.5 Hz increments. A total of 1000 measurements were conducted in an iterative ij cycle. The outcomes of the third test cycle are summarized in Figure 8 and Table 3.

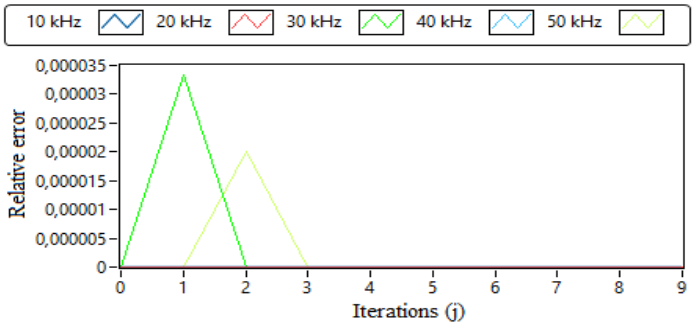

Figure 8. *The third test results of the search algorithm*

Table 3

Relative error values [%] in the 3rd test cycle

Δf: \ f_s:	**10 kHz**	**20 kHz**	**30 kHz**	**40 kHz**	**50 kHz**
1	0	0	0	0	0
2	0	0	0.0033	0	0
3	0	0	0	0	0.002
4	0	0	0	0	0
5	0	0	0	0	0
6	0	0	0	0	0
7	0	0	0	0	0
8	0	0	0	0	0
9	0	0	0	0	0
10	0	0	0	0	0

5. Conclusion

In a line scan camera-based measurement system, the optimal frequency of the lighting control signal can be determined by analyzing the average and variance values of the vector containing the overlap ratios between the exposure signal and the lighting control signal. The developed search algorithm can be utilized to identify the point where the maximum average value and minimum variance value of the vector represent the ideal frequency.

The application of the algorithm not only determines the optimal lighting frequency but also enhances the stability of the system. During testing, the search process demonstrated accurate frequency adjustment, even when there was a significant initial discrepancy between the exposure signal and the lighting control signal. By identifying the optimal frequency based on the average and variance, the method effectively minimizes intensity fluctuations and improves image quality.

As a result, machine vision-based measurement systems can capture more precise data, which is critical in industrial applications.

Future research could extend the algorithm's applicability to operate under various environmental conditions, such as changing lighting environments or the use of different camera types. Furthermore, future developments may explore the real-time implementation of the algorithm, allowing automated systems to respond more quickly and accurately to environmental changes, thereby further enhancing the reliability and efficiency of machine vision-based systems.

References

[1] Forgacs, Z. and Trohak, A. (2022). A Measurement Method for Determining Speed of High-Speed Rotating Parts. *2022 23rd International Carpathian Control Conference (ICCC)*, IEEE, May 2022, 203–207. https://doi.org/10.1109/ICCC54292.2022.9805948

[2] Mosa, Z. M. and Akin, E. (2021). Design and sorting of an object identification on machine vision by using line scan camera. Technium: *Romanian Journal of Applied Sciences and Technology*, Apr. 2021, Vol. 3, No. 3, 100–112. https://doi.org/10.47577/technium.v3i3.3181

[3] Cognex Corporation. *A Practical Guide to Using the In-Sight 5604 Line Scan Vision System*. https://support.cognex.com/en/downloads/detail/in-sight/661/1033

[4] Basler A. G. Basler Line Scan Cameras. https://www.baslerweb.com/en-sg/cameras/line-scan-cameras/

[5] Kumar, V. and Sudheesh Kumar, C. P. (2020). Investigation of the influence of coloured illumination on surface texture features: A Machine vision approach. *Measurement*, Feb. 2020, Vol. 152, 107297. https://doi.org/10.1016/j.measurement.2019.107297

[6] National Instruments Inc. (2019). A Practical Guide to Machine Vision Lighting. https://www.ni.com/en/shop/choosing-the-right-hardware-for-your-vision-applications/a-practical-guide-to-machine-vision-lighting.html

[7] Basler A. G. (2019). *Basler racer USER'S MANUAL FOR GigE VISION CAMERAS*.

[8] Pal, S., Bhattacharyya, A. and Ray, R. (2021). Modified excluded volume hadron resonance gas model with Lorentz contraction. *Nuclear Physics A*, Volume 1010, 122177. https://doi.org/10.1016/j.nuclphysa.2021.122177